



HAL
open science

Cross-method identification of hydrogenated species originating from dibenzyltoluene/(benzyl)benzyltoluene in a promising commercial LOHC

C. Maudet, X. Ji, E. Louarn, F. Fache, L. Vanoye, C. Lorentz, L. Pitault, V. Meille

► **To cite this version:**

C. Maudet, X. Ji, E. Louarn, F. Fache, L. Vanoye, et al.. Cross-method identification of hydrogenated species originating from dibenzyltoluene/(benzyl)benzyltoluene in a promising commercial LOHC. *Fuel*, 2025, 385, pp.134033. 10.1016/j.fuel.2024.134033 . hal-04913138

HAL Id: hal-04913138

<https://hal.science/hal-04913138v1>

Submitted on 27 Jan 2025

HAL is a multi-disciplinary open access archive for the deposit and dissemination of scientific research documents, whether they are published or not. The documents may come from teaching and research institutions in France or abroad, or from public or private research centers.

L'archive ouverte pluridisciplinaire **HAL**, est destinée au dépôt et à la diffusion de documents scientifiques de niveau recherche, publiés ou non, émanant des établissements d'enseignement et de recherche français ou étrangers, des laboratoires publics ou privés.



Distributed under a Creative Commons Attribution 4.0 International License



Full length article

Cross-method identification of hydrogenated species originating from dibenzyltoluene/(benzyl)benzyltoluene in a promising commercial LOHC product

C. Maudet^{a, b, 1}, X. Ji^{a, b, 1}, E. Louarn^{b, c}, F. Fache^d, L. Vanoye^e, C. Lorentz^b, I. Pitault^{a, b, *}, V. Meille^{b, 1, *}

^a LAGEPP, CNRS, Université Claude Bernard Lyon 1, 43 Boulevard du 11 Novembre 1918, 69622 Villeurbanne, France

^b IRCELYON, CNRS, Université Claude Bernard Lyon 1, 2 Avenue Albert Einstein, 69626 Villeurbanne, France

^c ICP, CNRS, Université Paris-Saclay, 14 avenue Jean Perrin, 91400 Orsay, France

^d ICBMS, CNRS, Université Claude Bernard Lyon 1, 1 Rue Victor Grignard, 69100 Villeurbanne, France

^e CP2M, CNRS, Université Claude Bernard Lyon 1, CPE Lyon, 43 Bd du 11 Novembre 1918, F-69616 Villeurbanne, France

ARTICLE INFO

Keywords:

LOHC
Isomer
Hydrogenation
Mass spectrometry
Dibenzyltoluene
Molecular balance

ABSTRACT

A commercial heating fluid, called with the generic name “DBT”, composed of different isomers of dibenzyltoluene (DBT) and of (benzyl)benzyltoluene (BBT), is known as a potential Liquid Organic Hydrogen Carrier (LOHC). The analysis of the hydrogenated mixtures was performed using gas chromatography alone (GC-FID) or coupled with mass spectrometry (GC-MS). The hydrogenated compounds used for the analysis were obtained by the hydrogenation of the commercial mixture at 150 °C. The identification of all the isomers originated from DBTs was achieved studying specific fragmentation observed in electronic ionization (EI) mass spectra. The distinction between hydrogenated DBTs and BBTs was also obtained. The isomer distinction was further supported by the molecular balances established during hydrogenation experiments carried out at 150 °C. 2,3-DBT and 3,4-DBT were synthesized and hydrogenated individually to facilitate the identification of their hydrogenated compounds, which showed certain inversions in the chromatograms. For the BBT isomers, the identification of each individual isomer is not confirmed, mainly due to overlap of compounds under GC peaks. However, the degree of hydrogenation of all the BBT derived compounds was determined.

1. Introduction

Among the various ways of storing hydrogen, the use of liquid organic hydrogen carriers (LOHCs) is becoming increasingly important. It consists of using hydrogen-lean molecules that can store hydrogen through catalytic hydrogenation. The hydrogen is released (later or further) by catalytic dehydrogenation of the hydrogen-rich compound. Benzyltoluene (BT) and dibenzyltoluene (DBT) are the most studied LOHC compounds today because (1) they are liquid in a wide temperature range (−55 to 285 °C for BT and −34 to 386 °C for DBT), (2) they have a high hydrogen storage capacity (6.2 wt-%), and (3) they are available in high tonnage (widely used as heat transfer fluids) [1,2].

Nevertheless, these compounds do not exist as pure isomers but as mixtures that deserve to be studied as the isomers may have different reactivity to hydrogenation and dehydrogenation and may impact the performance of the hydrogen storage process. Concerning BT, the most widely used commercial product is the Marlotherm LH[®] containing 3

isomers. These isomers were synthesized individually by Kim et al. [3], which showed that the *para* isomer had faster H₂ storage and release rates than the *ortho* and *meta* ones. Commercial DBT products under the tradename Jarytherm[®] or Marlotherm SH[®] gather 15 compounds, 9 of which have the methyl group on the side aromatic cycle ((benzyl)benzyltoluene - H0-BBT) and 6 of which have the methyl group on the middle cycle (dibenzyltoluene - H0-DBT). This isomer mixture is therefore named H0-DBT/BBT in this publication. The identification of all the H0-DBT/BBT compounds has been the subject of a previous work and has been published by our group [4]. Similar results have also been found recently by Jeong et al. [5]. The hydrogenation of the H0-DBT/BBT mixture yields H6-DBT/BBT, H12-DBT/BBT and H18-DBT/BBT lumps, with the addition of 6, 12 and 18 hydrogen atoms on, respectively, 1, 2 and 3 cycles. The ring preference during hydrogenation was first explored by Do et al. [6] using ¹H NMR by only

* Corresponding authors.

E-mail addresses: isabelle.pitault@univ-lyon1.fr (I. Pitault), valerie.meille@ircelyon.univ-lyon1.fr (V. Meille).

¹ First author.

considering the 6 H0-DBT compounds. It was found that the hydrogenation of H0-DBT has a side-side-middle (SSM) reaction pathway over a Ru/Al₂O₃ catalyst but the preference over either one of the side rings has not been demonstrated. The side rings of H0-DBT species are different due to the relative positions of these rings and the methyl group on the middle ring. The hydrogenation of H0-BBT was studied by Jeong et al. [5] by synthesizing the *ortho*, *meta* and *para* (defined by the position of the aromatic group regarding the methyl group on the duo-substituted side ring) compounds and testing their hydrogenation rates individually. It has been found that the H0-BBT shows a 150 % faster reaction rate than the commercial H0-DBT/BBT mixture over Pt and Ru/Al₂O₃ catalysts [5]. Moreover, the configuration of isomers also has an influence on their adsorption onto catalyst active sites and thus showed an impact on the dehydrogenation reaction [7,8].

Knowing that the reaction rates (either for hydrogenation or dehydrogenation) depend on the relative positions of function groups in the isomers, the identification of all the compounds is required for detailed kinetic studies and for the eventual optimization of commercial products dedicated for hydrogen storage purposes. In this work, the identification of all Hx-DBT isomers and major Hx-BBT isomers was achieved using a combination of GC-FID, GC-MS, catalytic hydrogenation reaction molecular balance over commercial mixture, target organic synthesis of H0-DBT isomers and their individual hydrogenation.

2. Material and methods

2.1. Nomenclature

Hx-DBT/BBT lumps are named as it is and can be simplified as Hx, if no distinction between DBT and BBT compounds is needed, with $x = 0, 6, 12, 18$. The term “lump” used in this work represents a gathering of isomers with the same atomic composition and similar physico-chemical properties, e.g. the H6 lump represents the total of all the isomers that are H6. However, in order to distinguish the different isomers inside each lump, the following nomenclature of compounds is applied as demonstrated in Fig. 1 along with two examples for a clearer visualization, where Hx represents the total number of hydrogen atoms stored inside the molecule with $x = 0, 6, 12$ or 18 . For dibenzyltoluene and its related compounds, Sa represents the side ring that is closer to the methyl group on the middle ring and the number of hydrogen stored inside with $a = 0$ or 6 , Mb represents the middle ring containing the methyl group and the number of hydrogen stored inside with $b = 0$ or 6 , Sc represents the side ring that is further away from the methyl group and the number of hydrogen stored inside with $c = 0$ or 6 , α and β represent the relative position of the first Sa and second Sc side ring to the methyl group, respectively. For (benzyl)benzyltoluene and its related compounds, similar signification is applied except Sa represents the side ring that contains the methyl group, $S'c$ represents the side ring without the methyl group, α and β' represent the relative position of the middle ring Mb to the methyl group and the side ring $S'c$ to the first side ring Sa , respectively.

2.2. Chemicals and catalyst

Commercial H0-DBT/BBT mixture under the tradename Jarytherm™ (batch number: FT-21 054) was provided by Arkema. Commercial 5 wt-% Pt/C (Product name: Platinum, 5 % on carbon, dry, Product code: A11186, Lot number: 10218866) was purchased from Thermo Fisher Scientific and commercial 1 wt-% Pt/Al₂O₃ (Product name: Platinum on alumina, 1 wt-% loading, powder, Product code: 205966-25G, Lot number: MKCP4125) was purchased from Sigma Aldrich. n-Hexadecane (95 %, Product code: 43283, Lot number: M17G050) was purchased from Thermo Fisher Scientific. Toluene (Product code: 28676.297, Lot number: 17E104002) was purchased from VWR Chemicals. All chemicals and products were used without further treatment.

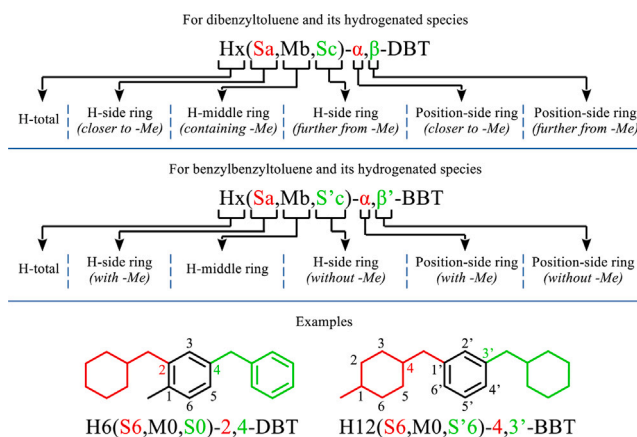


Fig. 1. Nomenclature for Hx-DBT/BBT isomers separating dibenzyltoluene, (benzyl)benzyltoluene and their hydrogenated species with examples.

2.3. GC-FID analysis

A Shimadzu GC (2010 GC-Pro) equipped with a FID detector and a DB-HeavyWax column (Agilent, 10 m × 0.1 mm × 0.1 μm) was used to carry out in-depth analysis of Hx-DBT/BBT compounds in the liquid samples. The injector temperature was set to be 250 °C with He as carrier gas, an injection volume of 0.1 μL and a split ratio of 10. The initial temperature of the column was 200 °C followed by a ramp of 20 °C min⁻¹ to 290 °C, which was held for 2 min. H0, H6, H12 and H18 lumps could be clearly separated according to different ranges of retention time and the majority of isomers inside the lumps except those in H18 could also be distinguished with high resolution. DB-HeavyWax column also allows shorter analysis times than other columns reported in the literature by a factor of 6 [9].

n-octadecane (n-C18) was applied as external standard for quantification of species. The RRFs (Relative Response Factors) of Hx isomers comparing to n-C18 are determined by experimental calibration with 20 artificial mixtures containing different quantities of each species. The same method used in GC-MS analysis was also applied to certain samples for a better separation and distinction of H6 and H12 isomers.

Another Agilent GC (6850 Network GC system) equipped with a FID detector and a HP-5 column (Agilent, 30 m × 0.32 mm × 0.25 μm), was used to separate light compounds from the heavy high-boiling Hx due to possible side reactions during hydrogenation reactions like cracking. The injector temperature was set to be 250 °C with He as carrier gas, an injection volume of 0.1 μL and a split ratio of 450. The initial temperature of the column was set to stay at 45 °C for 3 min, followed by a ramp of 20 °C min⁻¹ to 280 °C, which was hold for 5 min.

2.4. GC-MS analysis

GC-MS method has already been described in a previous article [4]. In brief, Fast GC-MS analyses were performed on a Shimadzu QP2010SE equipped with an Agilent HeavyWax column (10 m × 0.1 mm × 0.1 μm) in split-mode (carrier gas: H₂ - inj. vol. 0.2 μL - split ratio: 500). The GC temperature program was set as follows: 190 °C (0.5 min) then 15 °C min⁻¹ up to 220 °C (0.5 min) and finally 25 °C min⁻¹ up to 290 °C (0.3 min). Same method was applied to various samples under different energy of the electron beam from 20 to 70 eV in order to distinguish fragment ions generated by fragmentation and rearrangement.

GC×GC-TOF-MS (Agilent 6890N GCxGC, SepSolve TOF-MS, ZOEX cryogenic modulation system) analysis has also been carried out using: column 1 - VF1701 MS (30 m × 0.25 mm × 0.25 μm) and column 2 - DB1-MS (1.5 m × 0.1 mm × 0.2 μm). The temperature programs of the

two ovens are as follows: oven 1 – 100 °C (0 min) - ramp: 2.5 °C min⁻¹ to 180 °C & 1.2 °C min⁻¹ to 300 °C (10 min); oven 2 – 110 °C (0 min) - ramp: 2.5 °C min⁻¹ to 190 °C & 1.2 °C min⁻¹ to 310 °C (10 min).

2.5. Molecule synthesis

2.5.1. H0-DBT isomer synthesis

H0(S0,M0,S0)-2,3-DBT (2,3-dibenzyltoluene) and H0(S0,M0,S0)-3,4-DBT (3,4-dibenzyltoluene) were synthesized according to the method detailed in a previous publication [4]. 350 mg of H0(S0,M0,S0)-2,3-DBT and 480 mg of H0(S0,M0,S0)-3,4-DBT were obtained.

2.5.2. Catalytic hydrogenation

Catalytic hydrogenation reactions were carried out in a 300 mL stainless steel autoclave (Parr Instrument, Model Series 4560 Mini Reactors) batch reactor. For the hydrogenation of commercial H0-DBT/BBT mixture, a 0.015 mol-% Pt to reactant ratio was applied with the 5 wt-% Pt/C catalyst at 150 °C under 30 bar of H₂ with a stirring speed of 1000 rpm. And for the hydrogenation of synthesized single isomers of H0(S0,M0,S0)-2,3-DBT and H0(S0,M0,S0)-3,4-DBT which were diluted in n-hexadecane, a 0.5 mol-% Pt to reactant ratio was applied with the 1 wt-% Pt/Al₂O₃ catalyst at 250 °C under 30 bar of H₂ with a stirring speed of 1000 rpm. The reaction times were (1) 5 h for the hydrogenation of the mixture, (2) 14 h for the hydrogenation of H0-3,4-DBT, and (3) 6 h for the hydrogenation of H0-2,3-DBT. The reactor was purged 3 times by charging and discharging 30 bar of N₂ followed by 3 times of purging with 30 bar of H₂ prior to the start of heating. A sampling tube with a frit connected to the end was submerged into the reaction, allowing the gathering of liquid samples. When samples were gathered, the needle valve at the other end of the sampling tube on the head of the autoclave was opened and the pressure difference between inside the reactor (30 bar) and the exit of the sampling tube (1 bar) pushed the reaction liquid into the GC vials. The frit allowed the passage of the liquid and stopped the passage of catalyst particles. The liquid samples were further filtered by syringes and 1 μm filters to guarantee that there were no solid particles inside. The liquid samples were diluted in toluene with a mass concentration around 0.1 g mL⁻¹. Liquid phase samples taken during the reaction through the sampling tube were analyzed by 2 GC systems equipped with different columns (HeavyWax and HP-5), allowing the establishment of molecular balances over Hx species and possible side products.

2.6. Molecular balance

The quantity of a partially or fully hydrogenated species in each sample is determined by Eq. (1) where A_{H_x} represents the peak area of the species, A_E represents the peak area of the standard n-C18, m_E represents the mass of the standard in the analyzed sample, M_E represents the molar mass of the standard and M_{H_x} represents the molar mass of the concerned species. The RRFs of H0, H6, H12 and H18 lumps using the HeavyWax column are presented in Table 1. The RRFs of Hx isomers are supposed to be the same within each lump. No light compounds were observed using the HP-5 column during hydrogenation at 150 °C as shown in Figure S1 in the Supplementary Data. The only traces of molecules observed that were smaller than Hx species were the Hx-BT impurities that already existed in the H0 reactant. Therefore, it is reasonable to assume that there was no significant side reaction that took place which could influence the molecular balance of hydrogenation reaction.

$$n_{H_x} = RRF_{H_x} \frac{A_{H_x}}{A_E} m_E \frac{1}{M_{H_x}} \quad (1)$$

Since there were no loss in material due to side reactions during hydrogenation, at any given moment during the reaction, the total

Table 1

Relative response factors of H0, H6, H12 and H18 lumps. *The error of the experimental RRF of H6 was relatively high due to the fact that no pure H6 was available for the calibration.

Lump	H0	H6	H12	H18
RRF(exp)	1.05	0.95 ± 0.08	0.98 ± 0.02	0.99 ± 0.02
RRF(cal)	1.05	1.02	0.99	0.97

quantity of Hx lumps should stay constant and equal to the initial quantity of H0 added at the beginning of the reaction as shown in Eq. (2). Also as there were no isomerization occurring as side reaction, the same law applies to all the species originating from the same isomer i in H0 as shown in Eq. (3). The initial quantity of an isomer i being a constant, the sum of accumulation of each Hx species should follow Eq. (4). Therefore, by calculating the accumulation rate of each peak and applying a recursion routine pairing up species that meet the criteria using Python, some hydrogenated species could be identified.

$$n_{H_0}(t) + n_{H_6}(t) + n_{H_{12}}(t) + n_{H_{18}}(t) = n_{H_0}(t_0) \quad (2)$$

$$n_{H_0}^i(t) + n_{H_6}^i(t) + n_{H_{12}}^i(t) + n_{H_{18}}^i(t) = n_{H_0}^i(t_0) \quad (3)$$

$$\frac{n_{H_0}^i}{dt} + \frac{n_{H_6}^i}{dt} + \frac{n_{H_{12}}^i}{dt} + \frac{n_{H_{18}}^i}{dt} = 0 \quad (4)$$

3. Results and discussion

3.1. Mass spectra

Identification of each individual peak is a difficult task for isomers. Electronic Ionization (EI) however gives a genuine view of configuration of the species. In particular, it is possible to differentiate DBT from BBT, hydrogenation site for BBT and ortho-substituted species, thanks to site-specific McLafferty type rearrangements. The MS carried out under 70 eV provided crucial information for the identification of species. All mass spectra collected for different peaks are listed in the Supplementary Data. The 2D GC results and the corresponding mass spectra are presented in the Supplementary Data as well.

3.1.1. H6-DBT

Peaks due to H6-DBT are identified thanks to m/z 278 which corresponds to the molecular ion (Fig. 2).

The molecular ion can undergo numerous fragmentations:

(i) α -cleavage of the cyclohexane cycle (respectively methylcyclohexane for H6(S6,M0,S'0)- α , β' -BBT) leading to the formation of the m/z 195 ion (respectively m/z 181) and then the loss of 83 u (or respectively 97 u.) or α -cleavage between the two aromatic cycles forming m/z 173 after the loss of a xyllyl radical, which can only be observed for H6-BBT ;

(ii) other σ -cleavages leading to m/z 83 (or m/z 97) for instance ;

(iii) McLafferty rearrangement (McL) initiated from a 1,5-H' transfer from the cyclohexane to the central aromatic cycle (Fig. 3-path a) [10] promoting the loss of a cyclohexene (82 u) (or 96 u) and the formation of m/z 196 (or m/z 182);

(iv) a McLafferty-like rearrangement (McL') initiated from a 1,5-H' transfer from the CH₂ to the ipso-site of the side aromatic cycle (Fig. 3-path b), leading to the formation of the m/z 186 for H6(S0,M0,S'6)- α , β' -BBT and m/z 200 for H6(Sx,M0,Sy)- α , β -DBT and H6(S6,M0,S'0)- α , β' -BBT. The last two fragmentation paths (iii and iv) are highly structure-related and give information on the isomers involved.

The m/z 196 ion is observed on nearly all mass spectra of H6-DBT. It is due to any H6-DBT and to the H6(S0,M0,S'6)- α , β' -BBT. The m/z 196 formed ion is equivalent to a dimethylbenzylbenzene molecular ion. DBT-issued ions should be substituted on the same ring, forming a benzylxylene (BX), whereas BBT-issued ions should be substituted on

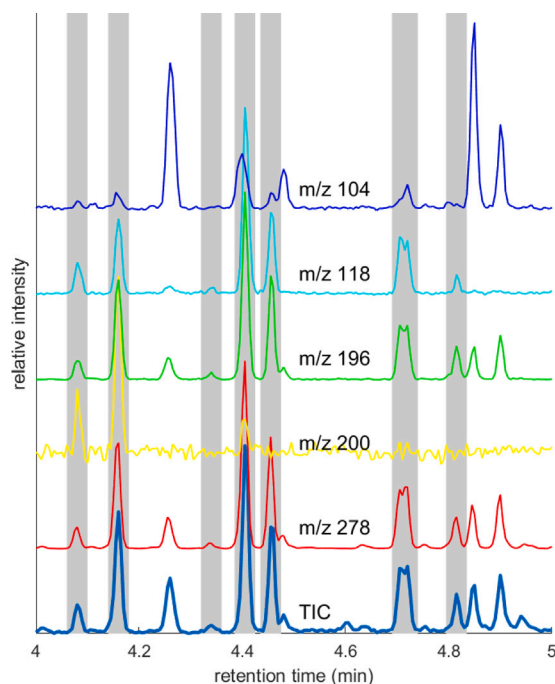


Fig. 2. GC-MS chromatogram of H6 products identified by the presence of the m/z 278 ion: total TIC and single ion monitoring of specific m/z (see text for more information). In gray, peaks identified as H6-DBT. The intensities are relative to the highest peak in the chromatogram.

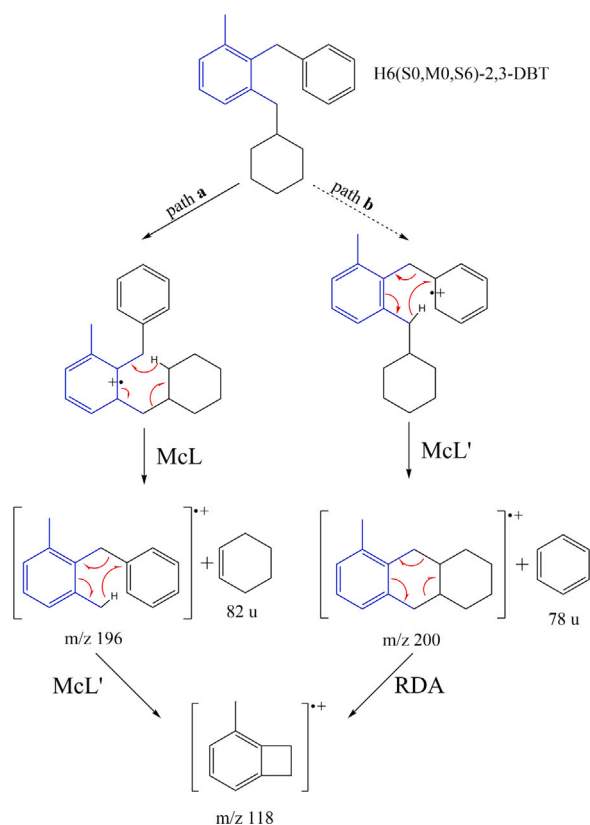
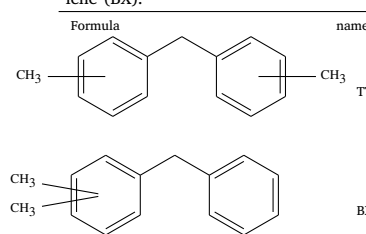


Fig. 3. MacLafferty (McL) and MacLafferty-like (McL') rearrangement paths for H6(S0,M0,S6)-2,3-DBT to the formation of m/z 196 by path a, m/z 200 by path b and m/z 104. They represent the fragmentation path noted respectively (iii) and (iv) in the text. The red arrows represent the hypothetical global reaction.

Table 2

Developed formula of the dimethylbenzylbenzene : tolyltoluene (TT) and benzylxylene (BX).



the two rings, leading to tolyltoluene (TT) (Table 2). These ions can undergo further fragmentation.

The base peak in the EI fragmentation spectra of the dimethylbenzylbenzene is, in the vast majority of the isomers, due to m/z 181, formed from the loss of a CH_3 (15 u) [11,12].

One notable exception is for the 2,2'-TT whose base peak is the m/z 104 ion. This ion is also one of the main fragments for 2,3'- and 2,4'-TT [11]. This ion is due to a McL' rearrangement highly favored in the case of an ortho-substituted species and to a lower extent for a para-substituted specie of TT molecules. Formation of the m/z 104 is then a label of a H6-BBT species, identifying peaks at $t_r = 4.26$ min, $t_r = 4.48$ min, $t_r = 4.90$ min, $t_r = 4.94$ min as probable BBT-candidates.

Similarly, BX-issued mass spectra present a peak at m/z 118. This peak is particularly significant for the 2,6-BX (40%) and for the 2,5-BX (28%), and the least probable for the 3,4-BX [12], and possibly none for the 3,5-BX. Presence of m/z 118 is observed prominently in the spectrum at $t_r = 4.08$ min, this ion is then probably due to H6(S0,M0,S6)-2,3-DBT.

As already observed for H0-DBT/BBT, ortho-substituted species can undergo McL' rearrangement (Fig. 3-path b for instance), leading to the loss of a benzene molecule (more for H6-DBT than for H6-BBT) or a toluene (for H6-BBT) and the formation of m/z 200 or m/z 186. It has to be noted, that these ions, such as tetralin, can further rearrange to m/z 118 or m/z 104, respectively, by a retro-Diels-Alder process. The ion m/z 186 is particularly prominent in the mass spectrum of the compound at $t_r = 4.26$ min. The m/z 200, though small, is only visible in the mass spectra of the two peaks at $t_r = 4.08$ and $t_r = 4.16$ min. The two ions result from a McLafferty-type rearrangement involving the two unsaturated cycles when situated in ortho positions, as in the dimethylbenzyltoluene and DBT/BBT spectra. Depending on the situation of the methyl, central for H6-DBT or side for H6-BBT, the product would then respectively be m/z 200 or m/z 186. The presence of the m/z 200 is then due to H6(S0,M0,S6)-2,3-DBT or H6(S0,M0,S6)-3,4-DBT [12].

Finally, ion m/z 165 is observed for all compounds up to 42% [11, 12]. This ion, such as m/z 181, is present on all the mass spectra.

These results allow to separate clearly the H6-DBT from the H6-BBT. Moreover, specific fragmentation paths give access to the possible identification of the individual species. As explained, the peak at $t_r = 4.08$ min is possibly H6(S0,M0,S6)-2,3-DBT whereas the peak at $t_r = 4.16$ min would be H6(S0,M0,S6)-3,4-DBT, or probably a mix of the two isomers H6(S0,M0,S6)-3,4-DBT and H6(S6,M0,S0)-3,4-DBT. From the m/z 118, we may determine that H6(S0,M0,S6)-2,4-DBT and H6(S6,M0,S0)-2,4-DBT correspond to the two peaks at, respectively, $t_r = 4.41$ min and $t_r = 4.46$ min. Finally, the two superimposed peaks at $t_r = 4.71$ min and $t_r = 4.72$ min could be due to H6(S0,M0,S6)-2,5-DBT and H6(S6,M0,S0)-2,6-DBT. Subsequently, H6(S6,M0,S0)-2,5-DBT would be at $t_r = 4.82$ min.

3.1.2. H12-DBT

In the GC-MS chromatogram (see Fig. 4), H12-DBT species are identified by their common molecular ion at m/z 284. Base peaks for the retention times corresponding to that criteria are either m/z 106 or m/z 120. The ion m/z 97 present in many spectra, which is sometimes the base peak, is mainly due to the formation of a deprotonated methylcyclohexane ion that stems from the σ -cleavage of the molecular ion in H12-BBT. Generally, in these mass spectra, the peaks are predominantly odd-electron species, indicating intense rearrangement reactions of the molecular ion.

Using the hypothesis that hydrogenation is occurring on the sides before the middle cycles in DBTs, it is possible to predict that the main fragmentation reaction should be a McLafferty rearrangement starting by the transfer of a 1,5-H[•] from one of the side cyclohexane to the middle aromatic cycle. This rearrangement leads to the unique formation of the m/z 202 ion by the loss of a cyclohexene for H12-DBT. H12-BBT, on the contrary, can lose either a cyclohexene or a methylcyclohexene leading to potentially both m/z 202 and m/z 188. Presence of a m/z 202 concomitant to the absence of m/z 188 is then a sign of the presence of a H12-DBT.

Moreover, depending on the original H12-DBT, ion m/z 202 may further rearrange by a similar McL process and lose the second cyclohexene, leading to the formation of the odd-electron m/z 120, equivalent to the molecular ion of the trimethylbenzene.

Each step of the double McL is favored in the case of the presence of a substitution on the ortho-position of the leaving cyclohexane cycle, with a preference over $\text{CH}_2\text{C}_6\text{H}_5$ on CH_3 . Therefore, the two molecules having the two side cycles in ortho-position (H12(S6,M0,S6)-2,3-DBT and H12(S6,M0,S6)-3,4-DBT) are more likely to have a large quantity of m/z 120 compared to m/z 202, followed by H12(S6,M0,S6)-2,6-DBT for which the two McL are equivalent. H12(S6,M0,S6)-2,5-DBT and H12(S6,M0,S6)-2,4-DBT should have a higher ratio of m/z 202 compared to m/z 120. Finally, H12(S6,M0,S6)-3,5-DBT have the two McL equivalent but in meta-position, then the molecular ion should be less fragmented than the other isomers.

Moreover, absence of m/z 97 and m/z 188 combined with the presence of m/z 202 is indicative of a H12-DBT. Attribution of the individual mass spectra is much more speculative. It is, however, reasonably possible from our MS results to make the assumption that the first H12-DBT ($t_r = 3.08$ min, $t_r = 3.25$ min) are H12(S6,M0,S6)-2,3-DBT and H12(S6,M0,S6)-3,4-DBT. H12(S6,M0,S6)-2,4-DBT is probably $t_r = 3.38$ min. H12(S6,M0,S6)-2,5-DBT and H12(S6,M0,S6)-2,6-DBT peaks seem to be completely merged at $t_r = 3.69$ min, as no other peak responds to the criteria of a H12-DBT spectra.

Meanwhile, the 2D GC-MS results have shown that there were small amount of H12 isomers that were below the quantification limit of GC-MS and GC-FID. Their mass spectra indicate that these small amount of isomers are produced from the hydrogenation of H0 with a side-middle step while the majority of the isomers are hydrogenated with the side-side ring preference. This implies that even though the side ring preference during the hydrogenation reaction with the commercial 5 wt-% Pt/C catalyst is predominant, the hydrogenation of the middle ring could still take place before that of the side ring.

3.1.3. H18-DBT

Many isomers are formed during hydrogenation process. All the H18-DBTs are identified by the mass of their molecular ion at m/z 290. The molecular ion is highly fragmented as expected from aliphatic compounds. Moreover, the mass spectra are very similar and little structural information is to be extracted from such mass spectra.

The base peak on all spectra is m/z 97. Three other main peaks are observed: m/z 193, m/z 179, m/z 111. The main difference lies in the presence or not of the m/z 179 peak. This ion is due to the formation of $[\text{C}_6\text{H}_{11}\text{CH}_2\text{C}_6\text{H}_{11} - \text{H}^+]$ ion, which can be explained from a direct cleavage of a H18-BBT molecule. On the contrary, a H18-DBT molecule would form the methylated equivalent m/z 193

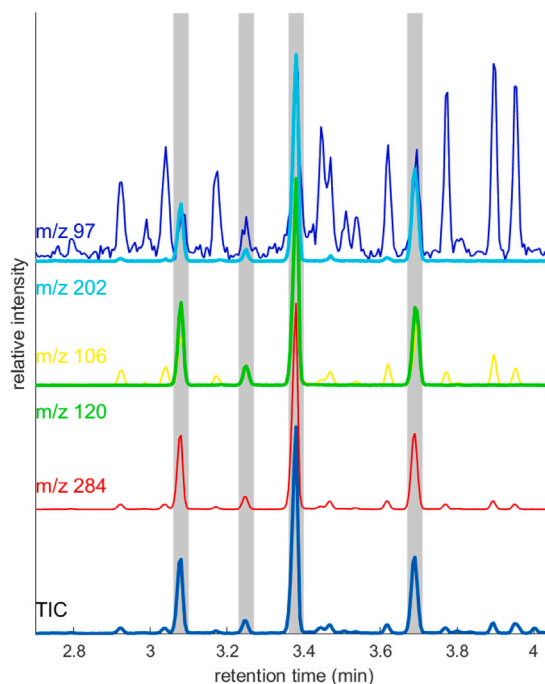


Fig. 4. GC-MS chromatogram of H12 products identified by the presence of the m/z 284 ion: total TIC and single ion monitoring of specific m/z (see text for more information). In gray, peaks identified as H12-DBT. The intensities are relative to the highest peak in the chromatogram.

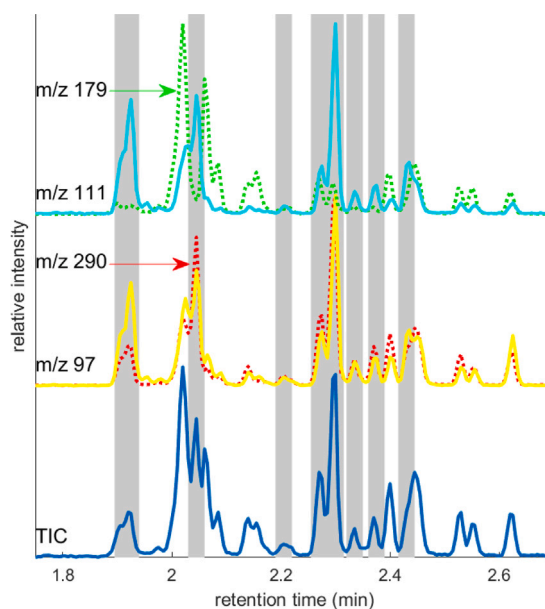


Fig. 5. GC-MS chromatogram of H18 products identified by the presence of the m/z 290 ion (molecular ion) and the base peak m/z 97: total TIC and single ion monitoring of specific m/z (see text for more information). In gray, peaks identified as H18-DBT. The intensities are relative to the highest peak in the chromatogram.

$[\text{CH}_3 - \text{C}_6\text{H}_{11}\text{CH}_2\text{C}_6\text{H}_{11} - \text{H}^+]$ ion, representing the loss of a side methylcyclohexyl radical. The m/z 193 can further fragment directly into m/z 97 on one hand or to m/z 111 on the other hand.

Fig. 5 presents the amount of these specific ions in the chromatogram. The ion m/z 179 clearly separates two types of molecules. It is present in the spectra of the H18-BBT compared to the H18-DBT.

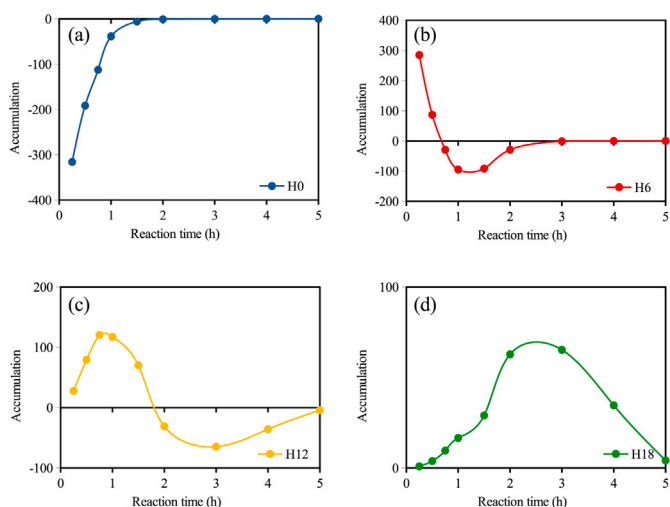


Fig. 6. Characteristic accumulation rate behavior of an H0 isomer and its hydrogenated species at 150 °C and 30 bar of H₂.

Therefore, the spectrum of a H18-DBT compared to a H18-BBT would have the presence of the *m/z* 193, a small to absent content of *m/z* 179, and a slightly higher amount of the *m/z* 111.

3.2. Hydrogenation molecular balance

For each H_x species inside the reactor, its variation of molar quantity vs. time or accumulation during hydrogenation could be expressed by $\frac{dn_{H_x}}{dt}$. The sign of the accumulation function reveals the nature of the behavior of the species with negative suggesting consumption and positive suggesting production. This function could be applied to different samples taken during hydrogenation for approximate estimation by slopes as shown by Eq. (5) where Δn represents the difference of quantity and Δt represents the difference of time between two consecutive samples. The shapes of accumulation curves are characteristic of the rank of molecules in the reaction schemes. Examples are given in Fig. 6, where the curves in Fig. 6(a), (b), (c) and (d) are characteristic of reactants (H0), primary products (H6), secondary products (H12) and tertiary products (H18), respectively. These curves played an important role on the identification of certain species in the border areas between different lumps or for lighter compounds as H_x-BT, where peaks tend to superpose.

$$\frac{dn_{H_x}}{dt} \approx \frac{\Delta n_{H_x}}{\Delta t} \quad (5)$$

For better visualization, an example of the chromatograms of the samples taken during hydrogenation is shown in Fig. 7. There are small overlaps of peaks in the interfaces between H_x lumps which are highlighted in gray. The attribution of these peaks into their corresponding lumps was achieved by the combination of MS spectra and their characteristic accumulation curves as mentioned above. Chromatograms zoomed in each H6, H12 and H18 lump are displayed in Fig. 8. The hydrogenation pathway of H_x species depends on the symmetry of the molecules. If the H0 molecule is asymmetrical, the first hydrogenation could take place on either one of the side rings which are not identical, generating thus two H6 molecules. But after the second hydrogenation step on the other side ring, there would only be one possible configuration for the H12 species. The last step of hydrogenation on the middle ring results in chiral carbon atoms which results in conformers and enantiomers and the number of corresponding H18 compounds therefore increases. On the other hand, if the H0 molecule is symmetrical, which is the case for H0(S0,M0,S0)-2,6-DBT and H0(S0,M0,S0)-3,5-DBT, the first hydrogenation would only yield

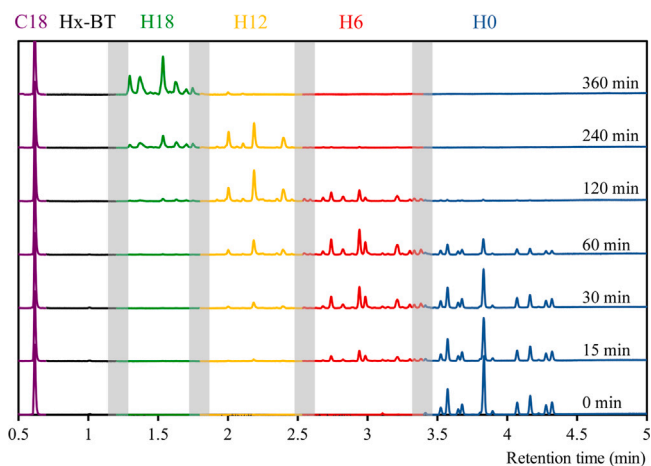


Fig. 7. GC-FID chromatograms of samples taken at different times (as indicated on the right side of the figure) during one hydrogenation experiment at 150 °C and 30 bar of H₂.

one H6 molecule as both side rings are identical. As for H0(S0,M0,S'0)-4,4'-BBT and its hydrogenated species, even if the molecule is symmetrical, since the two side rings are not identical, 2 different H6 compounds could still be obtained. The differentiation in hydrogenation pathway is demonstrated in Fig. 9. It is worth mentioning that among the 15 isomers in H0, 13 of them could potentially yield 2 different H6 each and 2 of them could only yield 1 H6, leading to a total of 28 H6 isomers. However only 14 peaks were observed in the chromatogram. This could be the results of the combination of peak overlap and the fact that the formation of some of the H6 isomers are not favored due to steric effects when the molecule is adsorbed onto the catalytic sites. Using the molecular balance method, multiple hydrogenated species have been identified like the H6(S6,M0,S0)-2,4-DBT at $t_r = 2.98$ min and H6(S0,M0,S6)-2,4-DBT at $t_r = 2.94$ min.

The orders of apparition of peaks corresponding to the species originating from a certain H0 are in general similar for each H6, H12 and H18 lump comparing to H0 with a few exceptions such as the case for Hx(Sa,Mb,Sc)-3,4-DBT and Hx(Sa,Mb,Sc)-2,3-DBT. The retention time of H0(S0,M0,S0)-3,4-DBT and H6(S0,M0,S6)-3,4-DBT is longer than that of H0(S0,M0,S0)-2,3-DBT and H6(S0,M0,S6)-2,3-DBT while the retention time of H12(S6,M0,S6)-3,4-DBT and H18(S6,M6,S6)-3,4-DBT is shorter than that of H12(S6,M0,S6)-2,3-DBT and H18(S6,M6,S6)-2,3-DBT. The hydrogenation of these two synthesized pure isomers, H0(S0,M0,S0)-3,4-DBT and H0(S0,M0,S0)-2,3-DBT further confirmed the attribution of H_x species as shown in Figure S2 in Supplementary Data. H0(S0,M0,S0)-3,4-DBT only gave one single H6 peak which could be an overlap of the two H6 isomers as also assumed by MS analysis. H0(S0,M0,S0)-2,3-DBT yielded two H6 compounds, of which the one with a longer retention time was much smaller in quantity. This is likely to be the consequence of steric encumbrance meaning that it is H6(S0,M0,S6)-2,3-DBT at $t_r = 2.68$ min and H6(S6,M0,S0)-2,3-DBT at $t_r = 2.83$ min. The peak at 2.83 min also contains mostly a H6-BBT species that overlaps with the H6(S6,M0,S0)-2,3-DBT.

3.3. Identification

By combining the results from MS spectra and hydrogenation molecular balance, the attribution of species are summarized in Table 3. All DBT species were successfully attributed and the distinction between DBT and BBT was clear. However, the attribution of BBT species was difficult to achieve due to the complexity of mass spectra and peak overlap for hydrogenation reaction. The error distribution on the molecular balance of isomers and both DBT and BBT families brought by such attribution for samples taken during one experiment

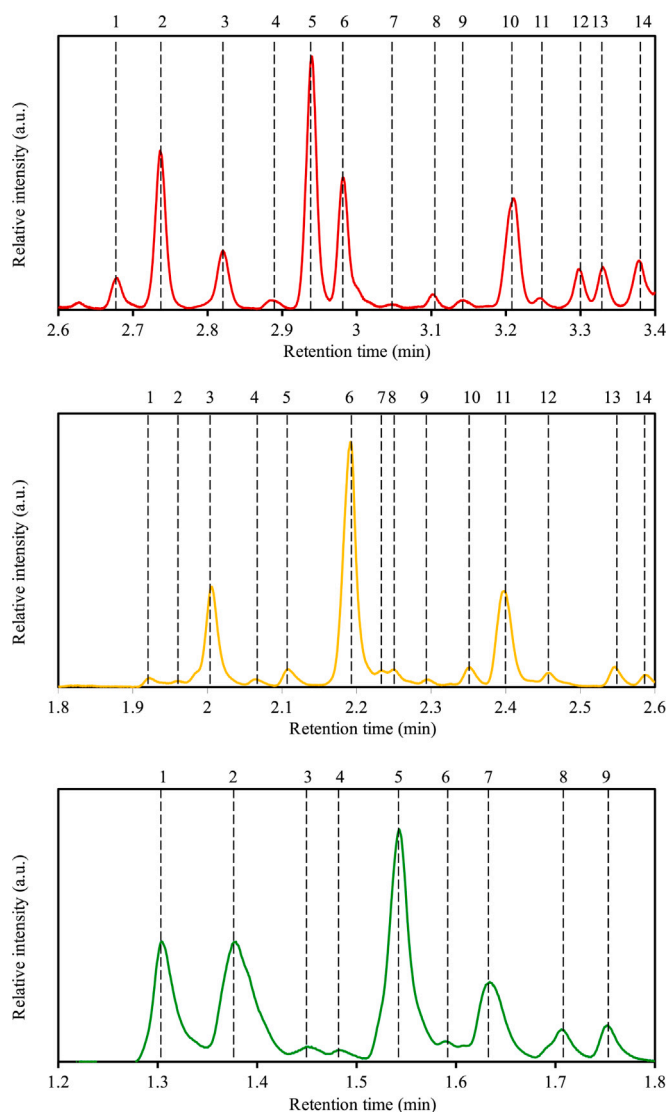


Fig. 8. Zoom-in on the top) H6, middle) H12 and bottom) H18 GC-FID chromatograms with numbers peaks in each lump.

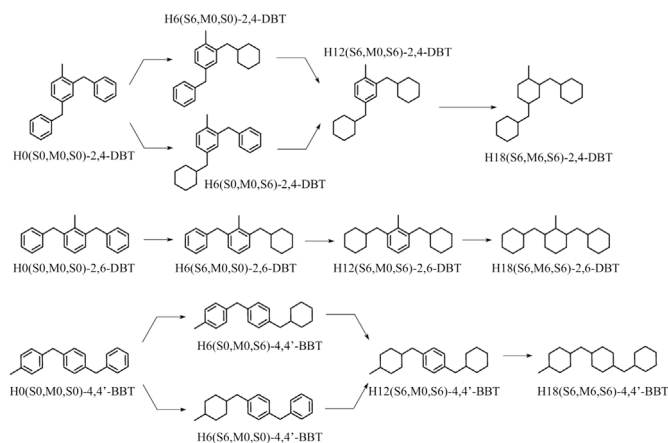


Fig. 9. Different reaction pathways as a consequence of molecule symmetry during hydrogenation.

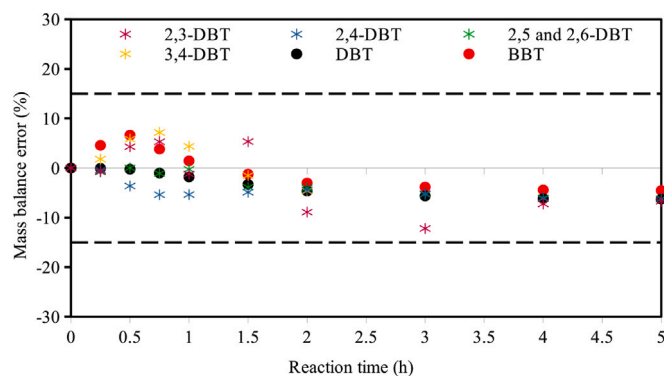


Fig. 10. Errors of molecular balances over each H0-DBT isomer and its hydrogenated compounds, the overall DBT and BBT, for samples taken during one hydrogenation experiment.

is demonstrated in Fig. 10 with an average value of -2.09% . Errors are calculated by the difference in molecular balance for each compound comparing to the initial quantity of the corresponding H0 isomer as shown in Eq. (6). This low error value could also support the results of attribution of the molecules. The isomer identification demonstrated that even though each unsymmetrical H0 isomer could potentially produce two different H6 isomers, the formation of one could be much less favored than the other as determined by kinetic or thermodynamic factors such as H0-3,4-DBT which only generated a single H6 isomer. The distinction of the compounds will open new gates for the mechanistic study of the hydrogenation reaction. The successful identification of these compounds will also be essential for the study of the behaviors of single isomers during hydrogenation.

$$\text{Error (\%)} = \frac{(n_{H18}^i + n_{H12}^i + n_{H6}^i + n_{H0}^i) - n_{H0}^i(t_0)}{n_{H0}^i(t_0)} \times 100 \% \quad (6)$$

3.4. Isomer reaction rates

The normalized initial reaction rates within the first 15 min of different H0-DBT and H0-BBT isomers at 150, 200 and 250 °C are listed in Table 4. The rates were obtained following Equation (7) where $n_{H0}^i(t)$ represents the quantity of the H0 isomer i after 15 min of reaction, $n_{H0}^i(0)$ represents the quantity of the H0 isomer i at the beginning of the reaction and t represents the reaction time which was taken to be 0.25 h. The normalized rates were applied in this work instead of the conventional reaction rates because the latter depend on the concentrations of the reactants, which were very different for each isomer, whereas the former could nullify the effect of concentration to better reflect the isomer activities.

$$r = \frac{n_{H0}^i(t) - n_{H0}^i(0)}{n_{H0}^i(0) \cdot t} \quad (7)$$

The missing data in the table were due to the fact that these isomers were in small quantities and rapidly went below the quantification limit of the GC. It can be observed that the reactivities of the vast majority of the isomers follow the same order at different temperatures and the few abnormalities were actually due to the small molar fraction of the corresponding isomers which introduced larger standard deviation. The reactivity of the compounds increased with the rise of temperature. The most reactive compounds are the ones whose benzyl rings are further away from each other. For H0-BBTs, the most active isomers were the H0-3,4' and H0-4,4'-BBT, both of which have the two encumbered groups on the *para* positions. For H0-DBTs, the most active isomers

Table 3

Attribution of peaks and species over GC-FID chromatogram combining the results of MS analysis and hydrogenation mass balance. * probable mix of two isomers (S6,M0,S0) and (S0,M0,S6). # the isomer could not be identified.

H6		
Peak number	Major compound	t_r (min)
1	H6(S0,M0,S6)-2,3-DBT	2.685
2	H6(Sx,M0,Sy)-3,4-DBT*	2.744
3	H6-BBT#	2.829
4	H6(S6,M0,S0)-2,3-DBT	2.891
5	H6(S0,M0,S6)-2,4-DBT	2.945
6	H6(S6,M0,S0)-2,4-DBT	2.988
7	H6-BBT	3.057
8	H6-BBT	3.109
9	H6-BBT	3.152
10	H6(S6,M0,S0)-2,5-DBT	3.216
	H6(S6,M0,S0)-2,6-DBT	
11	H6-BBT	3.253
12	H6(S0,M0,S6)-2,5-DBT	3.306
13	H6-BBT	3.337
14	H6-BBT	3.385
H12		
Peak number	Attribution	t_r (min)
1	H12-BBT	1.929
2	H12-BBT	1.967
3	H12(S6,M0,S6)-3,4-DBT	2.011
4	H12-BBT	2.072
5	H12(S6,M0,S6)-2,3-DBT	2.114
6	H12(S6,M0,S6)-2,4-DBT	2.194
7	H12-BBT	2.246
8	H12-BBT	2.257
9	H12-BBT	2.302
10	H12-BBT	2.357
11	H12(S6,M0,S6)-2,5-DBT	2.403
	H12(S6,M0,S6)-2,6-DBT	
12	H12-BBT	2.464
13	H12-BBT	2.553
14	H12-BBT	2.595
H18		
Peak number	Attribution	t_r (min)
1	H18(S6,M6,S6)-3,4-DBT	1.309
2	H18(S6,M6,S6)-2,3-DBT	1.384
3	H18-BBT	1.455
4	H18-BBT	1.490
5	H18(S6,M6,S6)-2,4-DBT	1.545
6	H18-BBT	1.597
7	H18(S6,M6,S6)-2,5-DBT	1.641
	H18(S6,M6,S6)-2,6-DBT	
8	H18-BBT	1.712
9	H18(S6,M6,S6)-2,5-DBT	1.759
	H18(S6,M6,S6)-2,6-DBT	

were the H0-2,4 and H0-2,6-DBT. It could be clearly observed as well that when the two benzyl groups are in *ortho* positions, the reactivities of the molecules are lower. The slowest reacting molecules in the H0-DBT and H0-BBT lumps are H0-2,3-DBT and H0-2,2'-BBT, respectively, which are much lower than the other ones and are detrimental to the overall hydrogenation reaction.

4. Conclusion

The identification of most of the compounds observed during the catalytic hydrogenation of the H0-DBT/BBT commercial mixture was made possible thanks to an in-depth analysis of the mass spectra of the compounds coupled to the fine molecular balance of each isomer during its hydrogenation. While it was possible to identify all the hydrogenated isomers of H0-DBT, it was not possible to identify the hydrogenated isomers of H0-BBT. Mass spectrometry provided some clues, but identification of the BBT isomers could not be confirmed by

Table 4

Normalized H0 isomer initial reactivities.

H0-BBT			
Isomer	Reaction rate (h^{-1})		
	150 °C	200 °C	250 °C
H0-3,4'-BBT	-2.2 ± 0.2	-2.1 ± 0.4	-3.5 ± 0.5
H0-4,4'-BBT	-1.8 ± 0.2	-2.6 ± 0.1	-3.10 ± 0.02
H0-4,3'-BBT	-1.6 ± 0.7	-2.4 ± 0.3	/
H0-2,4'-BBT	-1.5 ± 0.1	-2.0 ± 0.1	-2.8 ± 0.1
H0-2,3'-BBT	-1.5 ± 0.3	-1.9 ± 0.4	-3.4 ± 0.6
H0-4,2'-BBT	-1.1 ± 0.1	-1.5 ± 0.2	-2.1 ± 0.2
H0-2,2'-BBT	-0.9 ± 0.2	-1.3 ± 0.2	-1.8 ± 0.2
H0-3,3'-BBT	/	/	/
H0-DBT			
Isomer	Reaction rate (h^{-1})		
	150 °C	200 °C	250 °C
H0-2,4-DBT	-1.87 ± 0.02	-2.44 ± 0.02	-3.22 ± 0.02
H0-2,6-DBT	-1.70 ± 0.06	-2.35 ± 0.08	-3.0 ± 0.1
H0-2,5-DBT	-1.38 ± 0.04	-2.05 ± 0.07	-2.8 ± 0.1
H0-3,4-DBT	-1.3 ± 0.2	-1.9 ± 0.2	-2.6 ± 0.2
H0-2,3-DBT	-0.9 ± 0.2	-1.5 ± 0.2	-2.0 ± 0.2
H0-3,5-DBT	/	/	/

molecular balances due to overlapping peaks. The analyses also showed that one of the hydrogenated 3,4-DBTs, H6(S6,M0,S0)-3,4-DBT and H6(S0,M0,S6)-3,4-DBT, was not present in the mixtures hydrogenated with the 5 wt% Pt/C catalyst used, or that the two isomers showed overlapping peaks. Moreover, for hydrogenated isomers of 2,3-DBT and 3,4-DBT, there was a shift on the chromatograms between H6-DBT and H12-DBT, confirmed by synthesis. Finally, this identification will enable the hydrogenation kinetics to be studied in detail, revealing the most reactive isomers, and providing data for further hydrogenation processes.

CRediT authorship contribution statement

C. Maudet: Investigation, Formal analysis. **X. Ji:** Writing – original draft, Methodology, Investigation, Formal analysis. **E. Louarn:** Writing – original draft, Methodology, Formal analysis. **F. Fache:** Resources. **L. Vanoye:** Resources, Formal analysis. **C. Lorentz:** Investigation, Resources. **I. Pitault:** Writing – review & editing, Supervision, Methodology, Formal analysis. **V. Meille:** Project administration, Methodology, Funding acquisition.

Declaration of competing interest

The authors declare the following financial interests/personal relationships which may be considered as potential competing interests: Valerie MEILLE reports financial support was provided by French National Research Agency. If there are other authors, they declare that they have no known competing financial interests or personal relationships that could have appeared to influence the work reported in this paper.

Acknowledgments

The authors would like to thank the CNRS, France for its support through the 80|PRIME call, specifically for the NOSY-H2 project, and the French ANR, France for its support of the SAFHYR project (ANR-21-CE50-0045). The authors also acknowledge ARKEMA for providing the Jarytherm mix.

Appendix A. Supplementary data

Supplementary material related to this article can be found online at <https://doi.org/10.1016/j.fuel.2024.134033>.

Data availability

Data will be made available on request.

References

- [1] Aakko-Saksa PT, Cook C, Kiviaho J, Repo T. Liquid organic hydrogen carriers for transportation and storing of renewable energy – Review and discussion. *J Power Sources* 2018;396:803–23. <http://dx.doi.org/10.1016/j.jpowsour.2018.04.011>.
- [2] Jorschick H, Preuster P, Bösmann A, Wasserscheid P. Hydrogenation of aromatic and heteroaromatic compounds – a key process for future logistics of green hydrogen using liquid organic hydrogen carrier systems. *Sustain Energy Fuels* 2021;5(5):1311–46. <http://dx.doi.org/10.1039/D0SE01369B>.
- [3] Kim TW, Jo Y, Jeong K, Yook H, Han JW, Jang JH, Han GB, Park JH, Suh Y-W. Tuning the isomer composition is a key to overcome the performance limits of commercial benzyltoluene as liquid organic hydrogen carrier. *J Energy Storage* 2023;60:106676. <http://dx.doi.org/10.1016/j.est.2023.106676>, URL: <https://www.sciencedirect.com/science/article/pii/S2352152X23000737>.
- [4] Ji X, Louarn E, Fache F, Vanoye L, Bonhommé A, Pitault I, Meille V. Analysis of dibenzyltoluene mixtures: From fast analysis to in-depth characterization of the compounds. *Molecules* 2023;28(9):3751. <http://dx.doi.org/10.3390/molecules28093751>, URL: <https://www.mdpi.com/1420-3049/28/9/3751>.
- [5] Jeong K, Yook H, Lee SH, Han HJ, Jung Y, Han S, Shin SY, Choi M, Kwon S, Lee JH, Kim S-J, Kim SM, Han JW, Park JH. Benzyl-methylbenzyl-benzene: Improving hydrogen storage and release performance of dibenzyltoluene based liquid organic hydrogen carrier. *Chem Eng J* 2024;488:150927. <http://dx.doi.org/10.1016/j.cej.2024.150927>, URL: <https://www.sciencedirect.com/science/article/pii/S1385894724024148>.
- [6] Do G, Preuster P, Aslam R, Bösmann A, Müller K, Arlt W, Wasserscheid P. Hydrogenation of the liquid organic hydrogen carrier compound dibenzyltoluene – reaction pathway determination by ¹H NMR spectroscopy. *React Chem Eng* 2016;1(3):313–20. <http://dx.doi.org/10.1039/C5RE00080G>.
- [7] Huynh N-D, Hur SH, Kang SG. Tuning the dehydrogenation performance of dibenzyl toluene as liquid organic hydrogen carriers. *Int J Hydrog Energy* 2021;46(70):34788–96. <http://dx.doi.org/10.1016/j.ijhydene.2021.08.039>, URL: <https://www.sciencedirect.com/science/article/pii/S0360319921031657>.
- [8] Ouma CNM, Modisha P, Bessarabov D. Insight into the adsorption of a liquid organic hydrogen carrier, perhydro-*i*-dibenzyltoluene (*i* = *m*, *o*, *p*), on Pt, Pd and PtPd planar surfaces. *RSC Adv* 2018;8(56):31895–904. <http://dx.doi.org/10.1039/C8RA05800H>, URL: <https://pubs-rsc-org.docelec.univ-lyon1.fr/en/content/articlelanding/2018/ra/c8ra05800h>.
- [9] Modisha PM, Jordaan JHL, Bösmann A, Wasserscheid P, Bessarabov D. Analysis of reaction mixtures of perhydro-dibenzyltoluene using two-dimensional gas chromatography and single quadrupole gas chromatography. *Int J Hydrog Energy* 2018;43(11):5620–36. <http://dx.doi.org/10.1016/j.ijhydene.2018.02.005>.
- [10] Kuck D. Mass spectrometry of alkylbenzenes and related compounds. Part I. Gas-phase ion chemistry of alkylbenzene radical cations. *Mass Spectrometry Rev* 1990;9(2):187–233. <http://dx.doi.org/10.1002/mas.1280090203>, URL: <https://onlinelibrary.wiley.com/doi/abs/10.1002/mas.1280090203>.
- [11] Laseter JL, Lawler GC, Griffin GW. Influence of methyl substitution on mass spectra of diphenylmethanes: Analytical applications. *Anal Lett* 1973;6(8):735–44. <http://dx.doi.org/10.1080/00032717308058727>.
- [12] Sun H-B, Li B, Chen S, Li J, Hua R. An efficient synthesis of unsymmetrical diarylmethanes from the dehydration of arenes with benzyl alcohols using InCl₃-4H₂O/acetylacetone catalyst system. *Tetrahedron* 2007;63(41):10185–8. <http://dx.doi.org/10.1016/j.tet.2007.07.093>.